THESIS

MODULATING TRANSLATION DYNAMICS WITH TUNABLE OPTOGENETIC PROTEIN RECRUITMENT

Submitted by

Gretchen M. Fixen

Department of Biochemistry & Molecular Biology

In partial fulfillment of the requirements

For the Degree of Master of Science

Colorado State University

Fort Collins, Colorado

Spring 2024

Master's Committee:

Advisor: Timothy Stasevich

Erin Nishimura

Jean Chung

ABSTRACT

MODULATING TRANSLATION DYNAMICS WITH TUNABLE OPTOGENETIC PROTEIN RECRUITMENT

Genes encoded in our DNA are fundamental to human health and well-being. Their imperative role requires tight regulation throughout their journey to becoming functional proteins. These regulations, when disrupted, have been linked to many neurodegenerative disorders and cancers, stressing the importance of deconvolving their components. Translation is one of the final steps in this journey that has been extensively explored, resulting in a recent technique developed known as nascent chain tracking (NCT) coupled with MS2 stem loop tagging. Using this technique, we can track translation dynamics in real-time and in live cells. Despite this, there are still limitations in spatially and temporally tracking the recruitment of translation effectors to translation sites and accurately measuring these dynamics. With the incorporation of optogenetic blue-light-sensitive proteins, we can generate inducible biomolecular condensates that recruit green fluorescent protein (GFP)-tagged proteins and our reporter mRNAs. Using this controlled test-tube-like environment, we can discover the direct effects ribosomal quality control proteins have on translation dynamics. A main quality control pathway involves ZNF598, GIGYF2, and 4EHP proteins that mediate translation control during ribosome stalling. We discovered that both GIGYF2 and 4EHP can be recruited to these clusters and co-localize with our active translation sites in live cells. Further exploration found that 4EHP alone cannot fully cause translation inhibition with our system. Despite this, we do see translation initiation occurring over time due to complex formation with HIF-2∝. However,

GIGYF2 has distinct effects on these kinetics that are variable. This tool, when optimized, will be able to describe different proteins' effects on translation kinetics in an isolated environment in live cells.

ACKNOWLEDGEMENTS

Many people within and outside the department have made my graduate school experience the best I could hope for and have fueled my passion to pursue more.

First and foremost, I would like to thank the Stasevich lab for helping me complete my master's within their lab. My special thanks go particularly to Tim for being a fantastic PI and showing me that you can always be excited about science. To my main mentor Gabe, I couldn't have completed anything without your unwavering support, but mostly your fierce friendship. You have changed the trajectory of my life in the best way possible, and I cannot thank you enough for everything that you have done to motivate me and boost my confidence in science (even when I did not deserve it). You are the best, and I can't imagine working in a lab without you.

Of course, outside of the lab, I have been supported by many friends. I would like to thank a few specific groups that have been a significant part of my journey. To my roommates, thank you for being there for a good laugh at night. To my ochem friends, thank you for the built-in family found just through a grueling class. To my Master's cohort, I never thought I would find a home in MRB, but you guys gave me that; thank you.

Finally, I would like to thank the love of my family. Mom, Dad, you taught me the importance of education and that if I have the opportunity to pursue more, I should do it. You taught me how to work hard for what I want and to never give up. And to my sisters, Allison and Kiersten, despite everything, somehow, we will always be there for each other; thank you for your unconditional love.

TABLE OF CONTENTS

Chapter 1- Introduction

1.1 Genetic expression and the central dogma

The central dogma drives the force of genetic expression and, in turn, governs cell function implicating disease. Throughout history the central dogma has been heavily explored. Since the mid 1900's when the central dogma was first discovered, researchers have scrambled to find an answer to the mystery of genetic expression. [1] From there, the main framework of the central dogma was found to be that DNA undergoes transcription to become mRNA and this mRNA undergoes translation to become functional protein. [2] Because of its importance in human health, translation, a fundamental step of the central dogma, is tightly regulated and, essentially, the critical step in gene expression. The encoded segments can dictate the efficiency of translation at its different stages. [3] Importantly, translation has three main stages that can be affected: initiation, elongation, and termination-- all of which can be regulated by protein factors still under investigation. [4] Initiation, an essential hurdle for translation, begins with the aid of multiple "helper" proteins known as initiation factors. Initiation can be broken up into 4 main steps, formation of the 43 S pre-initiation complex, recruitment of the 43S complex to the 5' end, scanning of the untranslated region (UTR), and assembly of the 80S ribosome. [5,6,7] In order for these factors to properly function in initiation, the mRNA must be processed accordingly to have a 5' cap and a poly(A) tail. [8] eIF2 aids in forming the 43 S pre-initiation complex, a sort of "priming" for the ribosome. The cap is subsequently bound by eIF4E, the cap binding protein which recruits the 43S complex. [9] A plethora of proteins are then recruited, such as: eIF4G and eIF4A to form the eIF4F complex. [10]. Each of these proteins have specific roles in recruiting, priming, scaffolding, and directing the ribosome and transcript to the right locations to begin translating. Scanning the transcript of the AUG sequence is typically mediated through the 5' UTR. eUF1A helps break up the structured region in the 5' UTR so the ribosome can load onto

the transcript. [11] Finally, the 60S subunit of the ribosome is recruited by eIF5. This is only after the initiation codon has been identified on the transcript. While this is a quick rundown of translation initiation, it is an incredibly complex process filled with many regulatory steps still being explored today.

Once the transcript has been loaded and prepped from initiation, the next step of translation is its elongation stage. This stage is incredibly dependent on the resident transcript's sequence and accessibility. [12] Within the large subunit of the ribosome are multiple sites in which tRNA passes through during elongation, which occurs in the 5' to 3 directions. The ribosome then processes 3 mRNA residues at a time known as codons. To begin, the Met-tRNA is aligned in the P-site (peptidyl). [13] The first codon of the ORF will then settle in the A-site (aminoacyl). As the ribosome moves down the transcript, the tRNA will move through to the final E-site of the ribosome before leaving the ribosome. This process is mediated by a plethora of regulatory proteins and GTP that help preserve the nascent chain and allow it to fold into a fully functional protein. [14] The kinetics of how this process functions is left to many different factors within the cell. Once the ribosome reaches a stop codon in the sequence it will pop off from the transcript releasing the nascent chain.

The terms "translation factors" and "ribosome-associated quality control proteins (RQC)" were coined to describe proteins involved in this regulation. These factors can either enhance or inhibit translation, thereby affecting the cell's function and overall health. Understanding what regulates translation dynamics is integral to comprehending the further implications of diseases that target general gene expression. One major challenge in translation research is the ability to kinetically analyze translation and recruit translation inhibitors to specific sites. Furthermore,

measuring their effects in real-time adds another layer of complexity to this task. Deconvolving this pathway will reveal what factors affect gene expression.

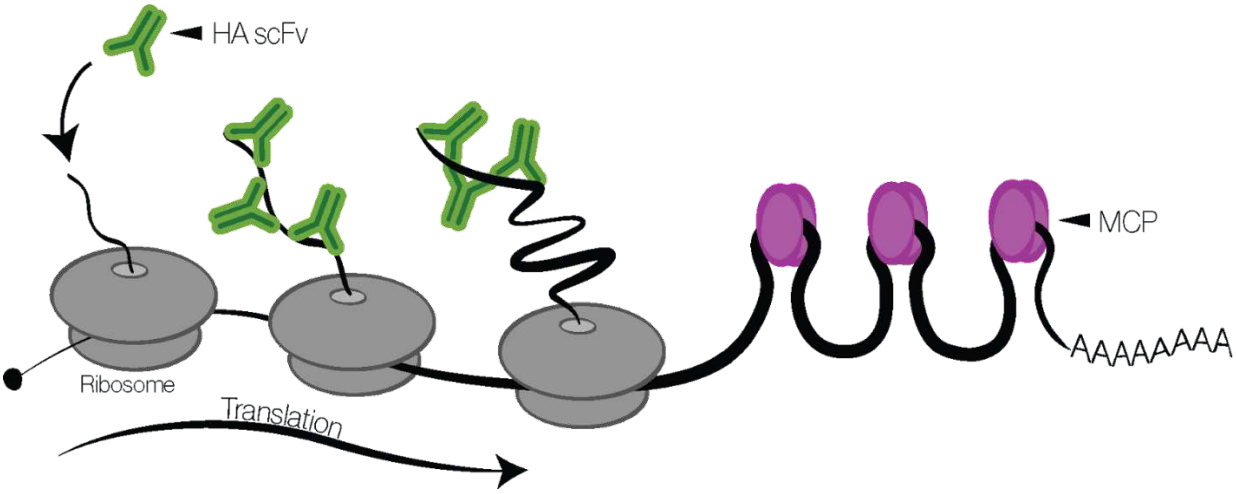

Figure 1: Nascent Chain tracking (NCT)
In green we have the HA scfV Frankenbody. In magenta we have the MS2 coat protein (MCP). This is a schematic for how NCT would look on a translating transcript.

1.2 Measuring translation dynamics

To address the challenge of measuring translation dynamics in real-time, researchers have developed single-cell imaging to view this process at a single-molecule level. Previously, translation dynamics were deconvolved through ribosome foot printing or profiling, which lacked the ability to measure translation dynamics in live cells in real time. An integral technique in the field discovered to combat this is Nascent Chain Tracking (NCT), developed by the Stasevich lab. This technique measures the real-time dynamics of single RNA translation in living cells at single-molecule resolution. Epitope tags, encoded for and subsequently positioned on nascent polypeptides of the reporter construct, recruit fluorescent antibody fragments (Fab) or Frankenbody scFVs, which are used to visualize the growing nascent chain as the ribosome moves across the reporter transcript. Simultaneously, a separate protein known as an MS2 coat protein (MCP) can bind to the MS2 stem loops at the end of our translating reporter mRNA. This

MCP can be stained due to its Halotag, and Fab or Frankenbodies can be added to the cells to bind our epitopes. The coupling of MS2-tagging and NCT allows for the observation of the stages of translation, in addition to tracking heterogeneity in translation dynamics. The addition of puromycin, an in and harringtonine helps validate these sites as active translation spots. NCT has revolutionized the visualization of translation dynamics in live cells. These reporter constructs can be altered depending on the gene placed between the two tagging components. Using this method, the previous difficulties of measuring translation kinetics and relating them back to gene expression can be solved. Certain additions to NCT have also increased its versatility, for instance, the spatial control over transcripts has been explored. This exploration began with implementing 5' BoxB stem-loops to develop a tethering assay, specifically with Argonaut protein found in P-bodies. Optimization of NCT provides continuous improvement to our understanding of gene expression and thus the direct effects of cell health. While tethering was able to be seen in live cells, a limitation of this technique is the lack of temporal control of translation and protein recruitment. Inability to catch every time scale of tethering leads to missed information that is integral to our understanding of translation.

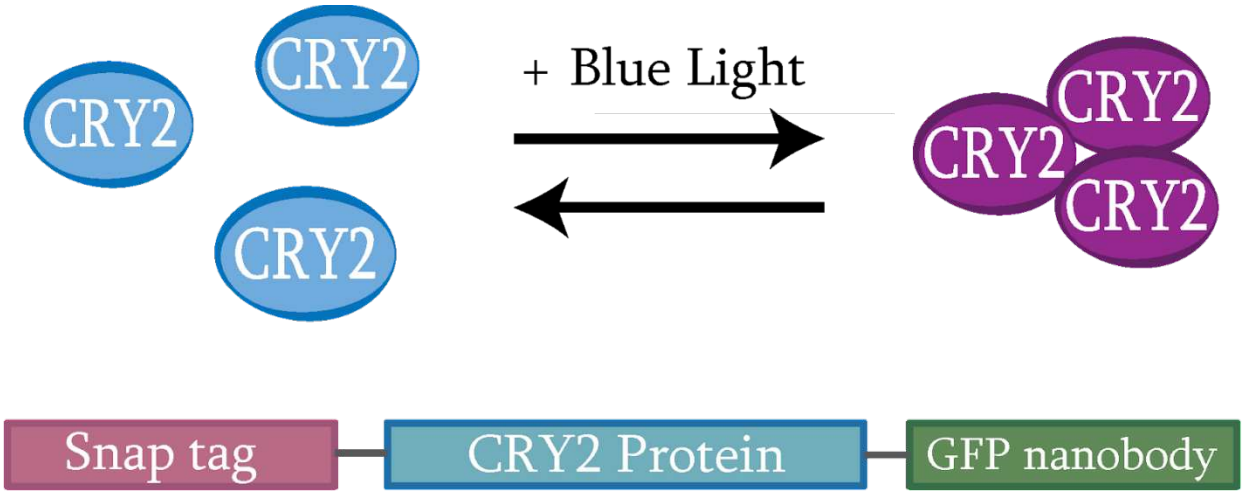

Figure 2: Cry2Olig clustering style and Construct
Cry2olig will oligomerize upon blue light exposure. This process is reversible when removing blue light. Below outlines the Snaptag in the 5' end of the Cry2 protein along with the addition of our GFP nanobody that will later promote tethering.

1.3 Optogenetic Protein Applications

Many different methods have been implemented to remedy the lack of temporal control in investigating translation. To control recruitment of transcripts, optogenetic technologies have been developed and applied. Optogenetic advances provide a promising remedy to NCT's weakness in temporal control [25]. This would be done by developing a recruitment method for our transcript to follow these proteins. The mechanism functions through the addition of a plant blue-light sensitive photoreceptor protein known as cryptochrome 2 (Cry2) [26]. Importantly, upon blue light exposure, Cry2 can form a homodimer as well as heterodimerize allowing for tethering. This function through blue light causing a conformational change within the Cry2 protein leading to rapid heterodimerization. This only occurs with the activation from blue light of 430-490 nm. [27] For example, an enhanced magnet system creates a measurable tethering event with the ability to recruit proteins and translation sites to designated areas. The enhanced magnet system is comprised of two Cry2 proteins that form a heterodimer [28] (Figure 2A)

A more biological application was found that Cry2 can form clusters which propagate through homodimerization [29]. Noticeably, these clusters create phase-separated condensates that do not incite a stress response. Initially, clusters were found to inhibit translation, but later experiments, in addition to our own, have shown residual translation signals [30]. To capture these signals, two main systems of clustering were developed to create phase-separated condensates: Cry2 LARIAT and Cry2olig wild-type [31] (Fig.2) These are all blue light inducible and each method vary in their strength of protein interactions, which affects how densely they form clusters and disrupt the translation environment. While cluster density differs, both systems do not fully shut down translation making them sufficient proteins to utilize in conjunction with NCT. Using these optogenetic proteins we will be able to create a local environment for our transcripts that is isolated from the rest of the cell, giving us a "test tube" in vivo. Using this specific phase separated technique, we can work to bridge the gap between in vivo and in vitro experiments and further apply this technique to different objectives. Since Optogenetic clusters are tetherable and don't fully disrupt translation, this will be applied to NCT to recruit known protein effectors to translation sites. Recruitment of these designated proteins to our Cry2olig clusters will interact with our translation signals and cause disruption [32,33]

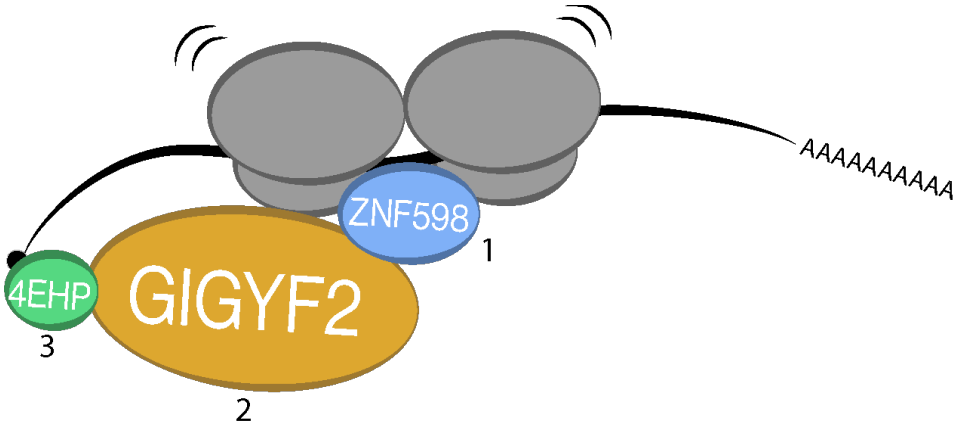

Figure 3: Proposed RQC pathway
In binding order:
1- ZNF598 → 2-GIGY2 → 3-4EHP

1.4 Recruitment of known translation effector proteins

There are many proteins that can inhibit translation due to the local environment they generate. Ribosome-associated quality control (RQC) proteins GIGYF2 and 4EHP are known regulators. [34,35] When ribosomes collide on transcripts, which occurs due to sequence specific structures in RNA, they cause stalling in elongation and ultimately produce truncated polypeptide chains, toxic to cell environments. [36,37] This toxic environment will ultimately lead to rapid cell death, which is something we want to avoid especially for certain cells that cannot regenerate themselves. One proposed alleviating pathway involves ZNF598's recruitment of GIGYF2 and then the subsequent recruitment of 4EHP which leads to translation inhibition. [38] 4EHP can bind to the 5' cap found on mRNAs and inhibit translation initiation, preventing the ribosome's ability to recruit and bind to mRNA [39]. 4EHP (eIF4E2) is also found to function as an initiation factor in hypoxic conditions within the cell. This occurs when HIF-2∝ complexes with 4EHP and can recruit initiation factors once more [40,41]. GIGYF2 is also multifaceted through its ability to recruit the Ccr4/NOT complex, another degradation pathway for mRNA. [41,42] All

of this will prevent a buildup of truncated chains after ribosome collisions. A schematic reveal how GIGYF2 and 4EHP function together in their signaling cascade (Fig.3). The main cause of this RQC recruitment is ribosome stalling, but this has not been tested in an isolated environment. Using both translation regulators we can visualize whether the protein's environment causes translational inhibition, or the protein itself causes translational inhibition. Ultimately, the goal is to further characterize the inhibition and requirements of our designated proteins while further validating our technique.

Due to the known limitations of NCT and MS2-tagging, we hypothesize that implementing our optogenetic system will allow for better characterization of translation dynamics due to its ability to isolate the transcript in the local environment. Therefore, our primary goals are to develop an optogenetic system that clusters with NCT, recruit RQC proteins to optogenetic clusters, and visualize translation shut-off over time following RQC recruitment. In addition, we hypothesize that the RQC protein pathway will still function without stalling of ribosomes and simply if recruited to translation sites. This will be determined on an individual protein basis.

Chapter 2: Applying Spatial and Temporal Control to Nascent Chain Tracking Through Optogenetic proteins

Rationale: Optogenetic proteins can sequester mRNA as found in previous publications. Due to this sequestration, nascent chains should subsequently be tethered as well due to mRNA recruitment. Despite papers claiming translational activity is inactivated through sequestration, preliminary data of preserved translation motivated us to pursue this recruitment further. This is an effective way to recruit mRNA and translation sites without the use of direct tethering which has variable effects on translation. It will simply recruit translation into the same generalized local environment in a phase separated means.

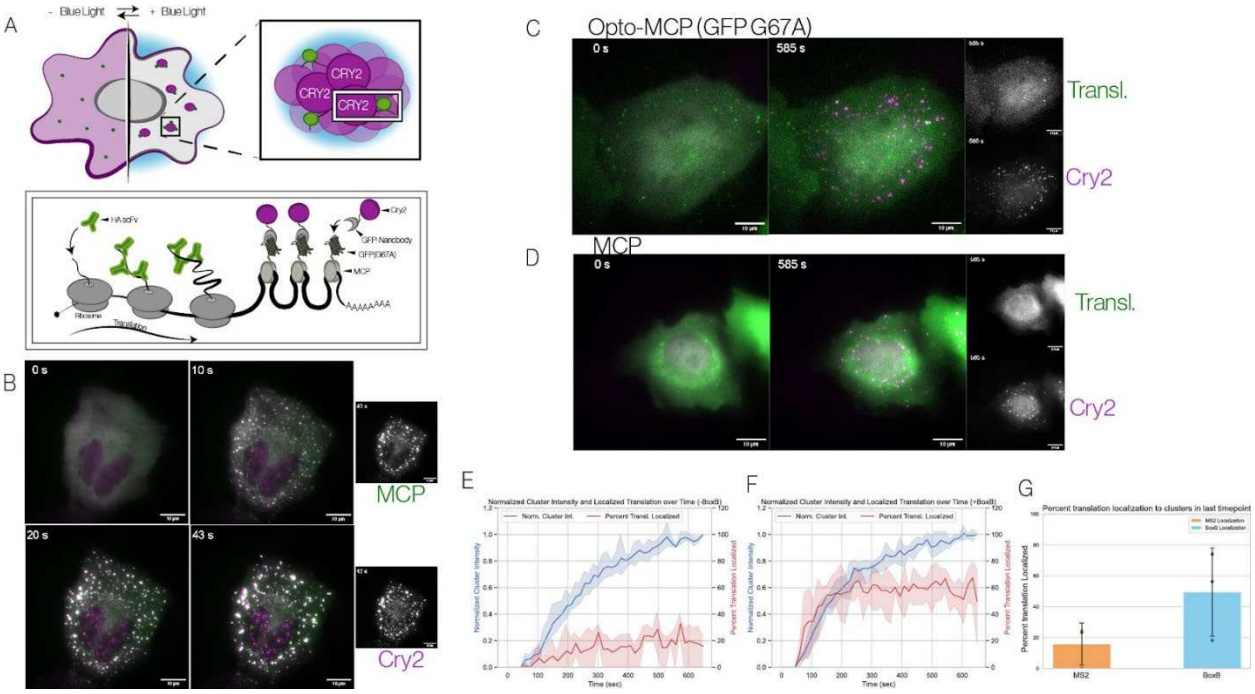

Figure 4 : Cry2olig's efficiency in our cell

A, Our model dictates how we are getting our system to work, from the cell level to the translation level. **B,** U2OS wildtype cells transfected with our Cry2olig plasmid, reporter transcript, and MCP. Consistent activation over 43 s. **C,** optogenetic MCP used (with non-fluorescent GFP), but not tagged, to visualize translation recruitment to clusters. **D,** MCP with no GFP, should not be tethered to the clusters over time because it lacks a GFP. **E,** cells using regular MS2 to colocalize with clusters, no GFP. This was plotted to show colocalization with clusters. **F,** Plot showing the tracking of mRNA using BoxB Halotag. **G,** comparison of colocalization at the end of the 10-minute time period. Percent colocalization is measured.

2.1: Recruitment of MCP and translation

To begin using optogenetic proteins as a technique for developing NCT, we needed to ensure that we could recruit our translation sites to these phase-separated clusters. Our system works by transfecting these components into various stable cell lines, specifically a stable cell line expressing Cry2olig. We can control when blue light is on to observe real-time cluster formation and interaction with our transcript. The model represents how and where we recruit our transcripts to our Cry2olig proteins (Fig. 1A). To validate this concept further, we tagged MCP with GFP and observed through blue light activation how quickly they co-localize if we place a GFP-nanobody on the Cry2olig protein. Within 10 seconds, consistent colocalization of MCP and Cry2olig protein is observed. This is evident through the splitting of our channels (Fig.1B). Having validated transcript recruitment, we moved on to visualizing recruitment of translation sites to these phase-separated clusters. We placed a non-fluorescent GFP on our MCP to visualize the colocalization of Cry2olig protein and translation sites. To measure the specificity of this mutated GFP (Opto-MCP, G67A), we tested MCP without GFP and with Opto-MCP and followed translation colocalization to clusters. We observed consistent recruitment of translation in cells transfected with Opto-MCP (Fig. 1C), which lasted throughout the imaging cycle after activation. Comparison with non-GFP MCP showed no lasting localization of translation (Fig. 1D), indicating higher mobility of translation and lack of colocalization in separated channel images. Subsequently, we tested mRNA localization, tracking regular MCP RNA over time and finding minimal colocalization (Fig 1E). Repeating the test with RNA including a BoxB stem loop stretch for tagging with Halotag showed rapid colocalization (Fig. 1F). Finally, we directly compared the percentage of localized vs. non-localized translation in our MCP control and BoxB transcripts at the last time point (Fig. 1G).

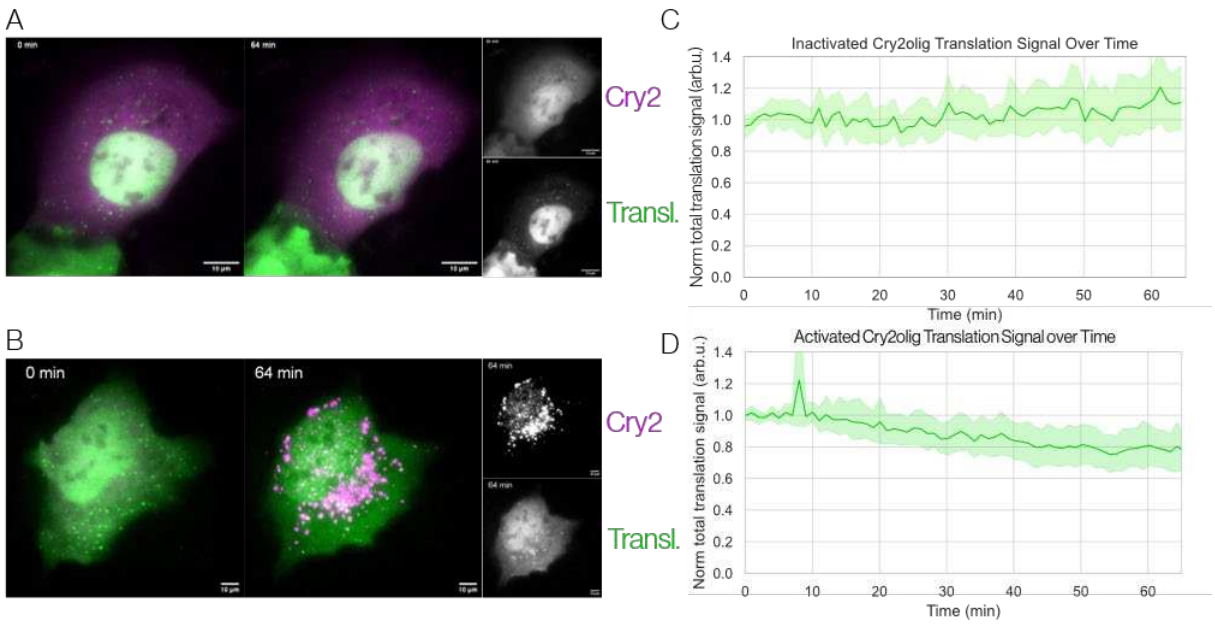

Figure 5 :Cry2olig effects on translation over time

A, U2OS wildtype cells transfected with the Cry2olig protein, KDM5B reporter transcript, and HA scFV-IRES-MCP plasmid. These cells were not activated over the 65 min time course.
B, U2OS wildtype cells transfected with the same components stated above. These cells were activated every 5 time points (5 minutes) over the 65 timepoint video.
C, graph tracking translation signal over time in our inactive Cry2olig images.
D, graph tracking translation signal overtime with active Cry2olig clusters forming.

2.2 Cry2olig's effect on translation over time

To assess whether Cry2olig integration would have a lasting effect on our cell's translation dynamics, the cells must be integrated with the proteins for longer periods of time. Firstly, we transfected our Cry2 protein within our cells and did not activate clustering. This means we had our blue laser covered over the course of the movie. After an hour we did not visually see lasting effects on our translation. (Fig 5A) Next, we repeated the transfection with wild type U2OS cells, however, this time we activated Cry2olig with a pulse of the 488 nm laser every 5 minutes over the course of a 60-minute video. From cluster activation, we did not visualize any lasting effects on translation (Fig. 5B). However, we do see consistent localization of translation to these clusters. To add quantification to our video analysis, we began tracking the translation intensity of each single-molecule site over time. Firstly, we addressed our inactivated cluster and did not see change from the normalized intensity over 60 minutes (Fig 5C). The normalized intensity considers the amount of starting translation sites compared to the ending number of translation sites and their combined intensity overtime. The graph indicates this intensity hovers around 1.0 indicating little to no change over time. This same quantification was done for our activated cells. Here, we get a similar result that lacked any significant difference from the starting intensity, only drifting slightly below 1 after nearing the 1-hour mark. (Fig 5D)

Chapter 3: Recruiting Ribosomal Quality Control Proteins to Active Translation Sites

Rationale: The RQC pathway can effectively shut down translation when stalling events occur on transcript. GIGYF2 and 4EHP can function as inhibitors without the first protein, ZNF598, in the signaling cascade. Previous studies have utilized direct tethering; however, it is unknown whether these proteins will function the same when placed in the same localized environment. Using the technique outlined previously utilizing optogenetic proteins, these RQC elements will be recruited to reporter transcript and translation dynamics can be effectively measured. These dynamics changes will be caught in real-time in live cells, never seen or done before. Using this technique, we will further deconvolve the pathway that, when disrupted, can lead to a plethora of neurological disorders.

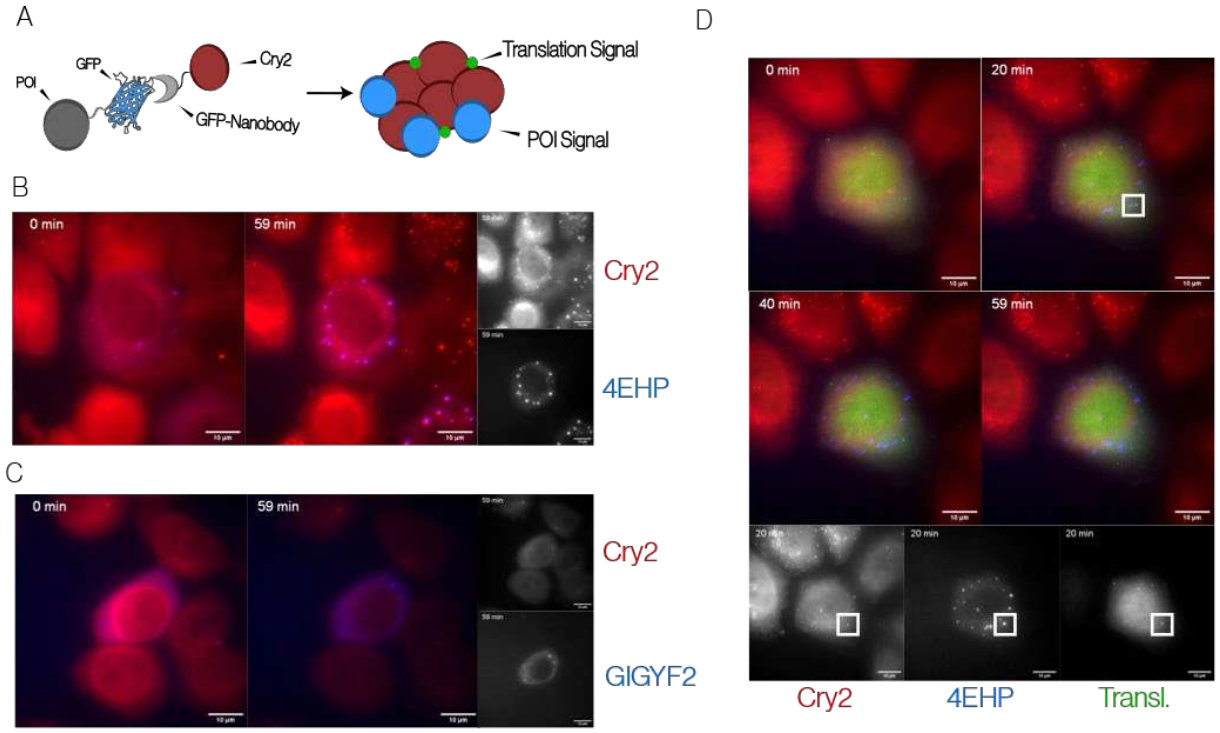

Figure 6: Validation of RQC protein recruitment to clusters and with translation

A, Schematic of protein recruitment to Cry2Ooig using GFP and GFP nanobody framework. **B,** Hela wildtype cells transfected with Cry2olig and the cap binding protein 4EHP, 60 minutes time course. **C,** Hela wildtype cells transfected with Cry2olig and the RQC protein GIGYF2, 60 minutes time course. **D,** Hela wildtype cells transfected with Cry2olig, 4EHP, reporter, and beadloaded with FAB and MCP.

3.1: Preliminary Tethering Control

To move forward with our deeper analysis of the RQC pathway, we required validation that this recruitment could occur within live cells and not disrupt any machinery. We recruit our protein of interests the same way our reporter transcripts are getting recruited, through the GFP and GFP nanobody. In this case, our GFP is left fluorescent on the protein of interest which is depicted by the given model (Fig 6A). This protein of interest will then colocalize, eventually, with translation. Initially, we transfected Cry2olig and 4EHP together and visualized their localization in Hela cells. They are consistently localizing at the beginning time point over the course of 60 minutes. The channels are split at the last time point to further validate the colocalization* (Fig 6B). Next, GIGYF2 was transfected along with Cry2olig and consistent localization is once again seen. The same visualization was used to show localization over time. (Fig6C). Finally, to assess the validity of this system, we must be able to recruit our POI and reporter transcript to localize translation and effector protein in the same cluster. This is seen for the first time in Hela cells validating that this system allows for the incorporation of all our components in addition to the fact they can all express enough to visualize in live cells (Fig 6D). Overall, this preliminary data allowed us to move forward with our experiments to better characterize this RQC pathway and kinetics in which they shut down translation with.

Early images do not have our two cameras aligned and colocalization is not exact

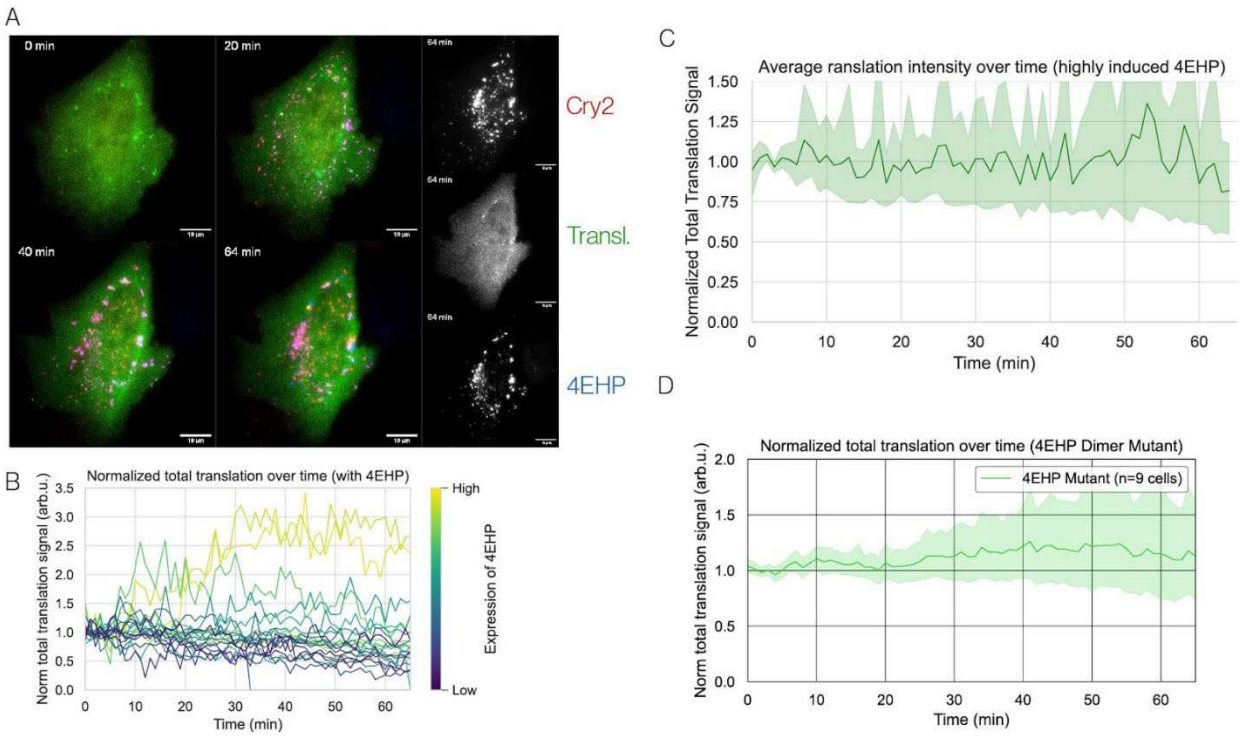

Figure 7: 4EHP Recruitment to Translation Sites

A, 65 timepoint, 1 minute interval movie depicting the recruitment of 4EHP over time. Last time point is separated into the three channels of visualization. **B,** Translation signals overtime per cell. Each cell is separated color-wise based on the expression of GFP. **C,** Average translation overtime in highly induced 4EHP cells. **D,** graph depiction of mutated 4EHP's effect on translation over time

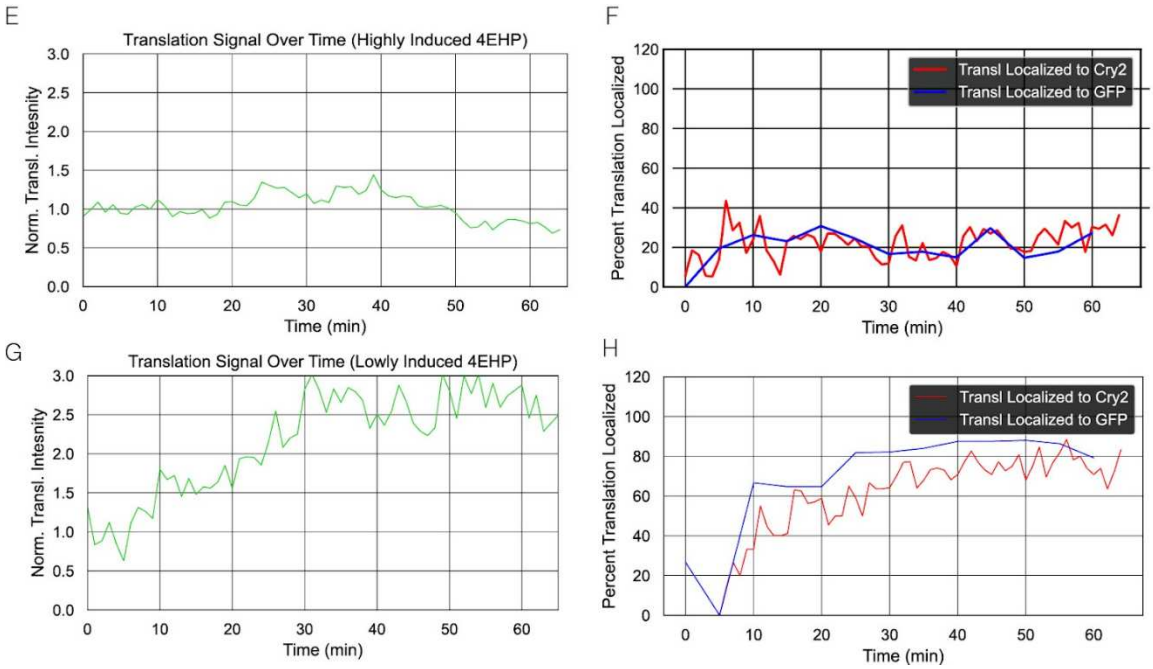

Figure 7: Continued

E, One's cell highly induced expression of 4EHP and its effects on translation over time. **F,** percent localization of translation to cry2olig clusters and with 4EHP. **G,** a lowly induced 4EHP single cell's effects on translation over time. **H,** subsequent localization of Cry2olig and 4EHP clusters over time.

3.2.1 Recruitment of 4EHP

We can successfully recruit 4EHP and translation sites to the same phase-separated localization. Over time, we can visually see translation sites do not go away after stable recruitment for 65 minutes. Instead, it appears like translation sites get brighter over time, in some cases. Some of these cells were treated with harringtonine to ensure that these are translation sites, however, there is still the possibility of stalling events, this is harder to track using any chemical inhibitor of translation. When plotted on a graph, we see there are significant amounts of cells that increase in translation intensity over time. To further characterize this trend, we investigated the GFP signal to sort via expression of 4EHP. From this, we found that higher expression of 4EHP led to higher signals of translation. This of course had to be optimized because too much 4EHP also led to no effects on translation, but less stable interaction indicating that there is a chance all the Cry2 proteins that mediate the recruitment are taken up by 4EHP protein. We can see that even with high amounts of 4EHP, there is still a variable response to translation initiation over time. This may be due to what was stated previously. (Fig 7C) Next, the dimer mutated version of 4EHP was explored. This mutant removes the binding interface to GIGYF2, the upstream binding of the initiation inhibition pathway. This graph reveals a higher likelihood of translation initiation; however, this is preliminary data that only has incredibly low expressing 4EHP within the cells. Further optimization of this will need to be tested. (Fig 7D) To further characterize localization of translation, further data analysis has been done on already acquired data. The first cell looked at was one of our highly induced 4EHP cells that had little to no effect on translation over time. (Fig 7E) When localization of translation to Cry2olig and 4EHP's GFP, little to no translation was localized. (Fig 7F) Next a cell with lowly induced 4EHP was investigated that had an extensive effect on translation over time leading to initiation. (Fig 7G). The percentage of localized translation sites to Cry2olig cluster and GFP clusters revealed

incredibly high colocalization compared to the previous graph. This would need to be done for every cell replicate to deconvolve a generalized trend.

*Last figure tracking over time

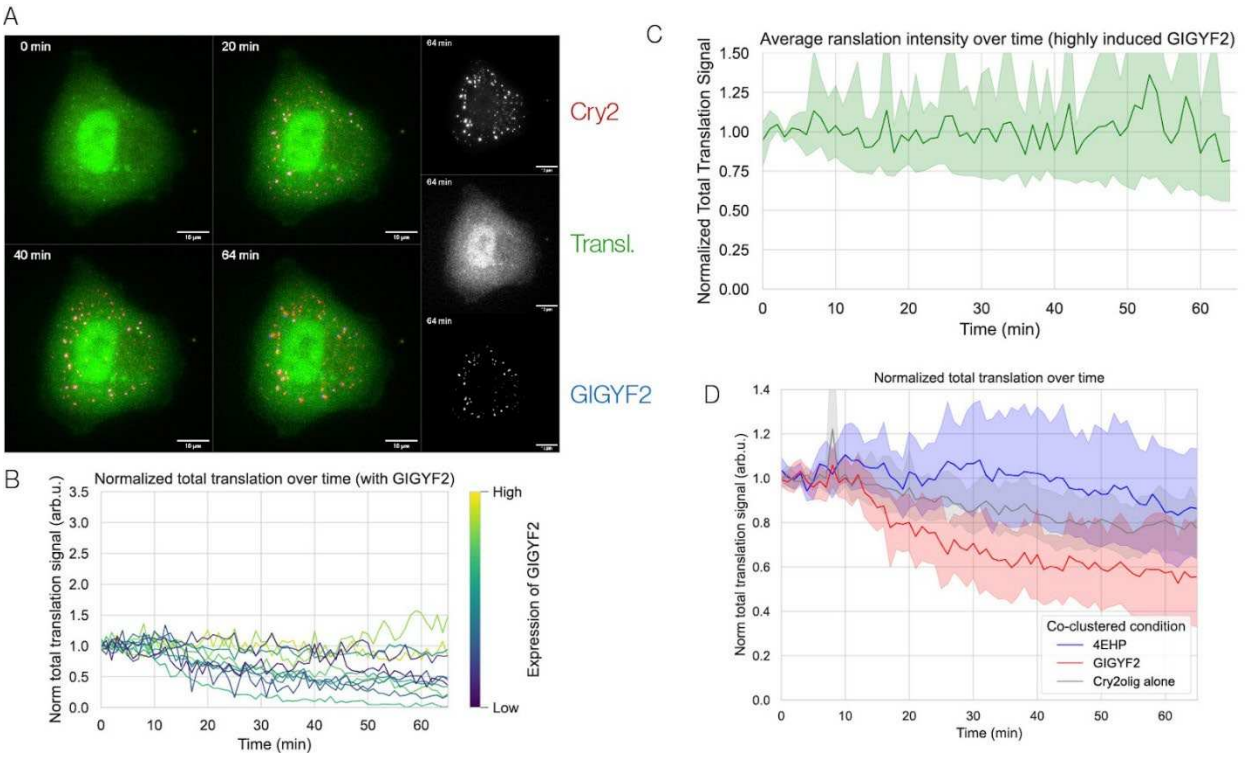

Figure 8: GIGYF2 Recruitment to Translation Sites

A, 65 minute, 1 minute time point video depicting translation over time. Last time point is split into the three channels as labeled. **B,** Translation overtime with GIGYF2 recruitment, each line is a cell and they are colored based on GFP expression. **C,** Highly induced GIGYF2 average translation signal overtime. **D,** combined 4EHP, Cry2Olig, and GIGYF2 translation averaged compared on the same graph.

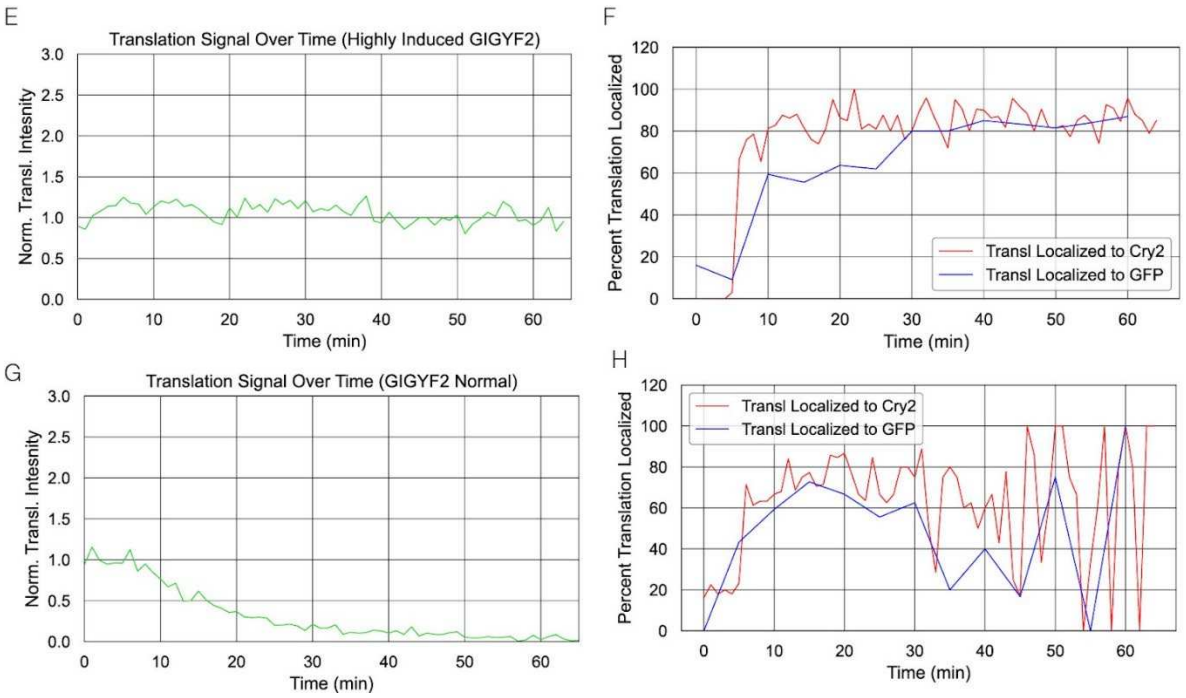

Figure 8: Continued

E, this is a single cell taken from our highly induced GIGYF2 cell. It has very little effect on translation over time. **F,** colocalization of translation to Cry2olig and GFP over time. **G,** Lowly GIGYF2 induced cell with a severe phenotype shutting down translation. **H,** Localization of translation to Cry2olog and GIGYF2 GFP over time.

3.2.2 Recruitment of GIGYF2 to clusters

The next protein we recruit is the protein upstream of 4EHP. Theoretically should be able to shut down translation because of its ability to recruit these inhibitory proteins. Our video of the cell shows consistent recruitment of GIGYF2 over time. These are visually interacting with the translation sites over the course of the 65-minute video. In addition, we can visually see translation shut down over time with this cell. This occurs within 20-30 minutes of the video. (Fig 8A) To further analyze these images we need to quantify the translation signal through its fluorescent intensity. This was done for all cells tested that visibly recruit GIGYF2. This graph left us with conflicting results since there was not a consistent drop in translation. In addition to this, it was not based on expression of the GFP indicating that GIGYF2 levels may not matter. This needs to be further assessed to provide a stronger conclusion. (Fig 8B). To assess the efficiency of GIGYF2's ability to shut down translation, we highly induced our inducible cell-line expressing GIGYF2. We could screen for this because high levels of GIGYF2 will phase-separate into a liquid-like condensate. Even with the high level of GIGYF2, we were unable to see consistent run off translation. (Fig 8C). Lastly, we compare all three conditions we are exposing our translation sites too. Despite GIGYF2's variable results, it still shuts down translation more than Cry2olig on its own and 4EHP. This means there is still a mechanism at play that allows it to function as an inhibitor more so than other proteins. (Fig 8D) Potentially translation will not be localizing to our Cry2olig clusters containing GIGYF2. To assess this localization, we measured the percent of translation over time colocalizing to translation sites and determining if this plays a role in the effects on translation. The first cell we looked at is a highly expressed GIGYF2 cell with little to no effects on translation upon clustering. (Fig 8E) The localization was measured, and percent of translation localization sits at around 80% indicating that there is some interaction with GIGYF2 and this interaction is not causing any

effects over time. The next cell was the lowly induced cells that had an intense effect on translation over time. This indication strikes a severe phenotype that is non typical. (Fig 8G) The localization was then measured to see if this would have further association and localization over time than the one not affected. This remained unchanged from the previous cell. The end of the graph is hard to read because of the rapid loss of translation over time. (Fig 8H)

Chapter 4: Discussion

Translation is a complex process and remains the critical step in the central dogma. Our lab has extensively explored the diverse effects on translation kinetics by developing NCT, a method to measure nascent chain production over time based on fluorescence intensity. Additions to this technique have been revolutionary in the field, such as generating a direct tethering assay with our reporter transcript using BoxB stem-loops. Through this technique, we have devised a way to recruit factors without direct tethering, which have unknown effects on transcripts. This was achieved using our optogenetic protein Cry2. With the technology described above, we can tether proteins of interest and our reporter transcript in the same localized environment. This technique allows us to create a phase-separated "test tube" within our cell. The novelty of this tethering enables us to better compare in vivo and in vitro experiments by effectively mixing controlled components that contain GFP (fluorescent or not). Optimizing this technique will lead to further controlled experiments with any proteins tagged with GFP. Moreover, using this technique to observe live dynamics provides us with more information than some direct tethering assays that screen transcripts the day after.

4.1 Aim 1

To achieve our objectives with this technique, numerous controls needed to be established. This was the focus of my first aim, which aimed to control when and which transcripts could be recruited. This began by developing an orthogonal technique that previously tethered mRNA to Cry2 proteins. Through this, we aimed to validate the method's ability to recruit using the GFP nanobody and be specific to our reporter transcript. This was confirmed through our first control, visualizing the MCP-tagged mRNA localized instantly with our clusters. This ensures that we know our transcript is being sequestered to these spots. For this system to work with NCT,

we needed to observe translation signals persisting over time to measure changing dynamics. Initially, we observed translation localization. This was tested by recruiting a second set of stem loops, BoxB, with a Halotag for staining to observe localization of translation to these mRNA clusters over time. We consistently observed localization of BoxB over time, with around 80% of transcripts being localized. This aligns with previous findings indicating that BoxB is not 100% efficient at tethering, thus replicating those findings. We also tested recruiting MS2 without a GFP tag, and these mRNAs did not recruit to clusters. This hypothesis was confirmed through analysis showing little to no localization to the clusters, validating that our clusters are specific to GFP-tagged components within the cell. This was further analyzed by comparing the last time point of localization using a bar graph, which showed that the BoxB transcript significantly recruits clusters more than just MS2.

The next part of my aim was to ensure that translation would not be shut down over time due to the presence and clustering ability of the Cry2 protein. Firstly, we tested whether simply transfecting Cry2 proteins into the cell without activating their clustering would disrupt translation. This was not observed visually in our videos, and upon further analysis of these videos, we did not observe any shut-down of translation over time. This was quantified on a single-particle basis over the course of 65 minutes. This test indicates that the expression of Cry proteins in the cell will not cause translation to shut down through a stress response. While the expression and quantity of Cry proteins are mostly controlled, there was a concern that integrating enough Cry2 to be activatable might be too much for the cells. Fortunately, this was not the case, so we moved forward with testing the effects of activated Cry2 over time. In our subsequent experiments, we once again did not visually observe any significant effects on our translation over time. This was quantified in the same manner, and we did observe a slight

drop-off in translation compared to the non-activated Cry2. This is likely since we tested the activated Cry2 more extensively than the inactivated Cry2. For a proper comparison, we should replicate our initial experiments more closely. Despite that, we can conclude that Cry2olig's clustering ability will not significantly disrupt translation over time, making it a great system to recruit factors and localize translation sites to our clusters.

4.2 Aim 2

My second focus was on recruiting known factors to the same area without causing too much disruption within the cells. There was a concern that Cry2 might be fully bound by the transcript before binding any protein of interest, among other worries. To direct our questions towards a biological process, we delved into the RQC pathway, which has been minimally explored and remains elusive. The general idea is that through recruitment, these factors should be able to shut down translation once localized. As mentioned earlier, this leads to translation initiation inhibition, which still occurs with just the recruitment of 4EHP or GIGYF2. We began testing this technique's validity by generating stable cell lines in Hela cells expressing either 4EHP or GIGYF2. The initial data confirmed that both, once GFP-tagged, could be recruited to translation sites. Further validation was conducted by integrating our NCT components to observe translation. This was once again observed, but in small amounts within these Hela cells. This indicates that these components are quite challenging to integrate even through transfection and bead loading. These initial experiments served as the necessary controls to ensure that this system would work effectively in the long run with all these components. While Hela cells were suitable for testing, we aimed to transition to U2OS cells, as they are the mainstay of our lab.

After developing these control results, we began the long work of generating stable cells in U2OS cells. This process was long and tedious, however, through the Piggybac stable cell

lines method, we were able to complete three stable cell lines each expressing their own protein: 4EHP, GIGYF2, and Cry2. The Piggybac system functions through integrating into transposons using transposases. Transposons are sequences within the genetic code that are moveable, and their expression is variable. Because of this, our stable cell lines have a lot of heterogeneity in expression of the proteins of interest. Despite this, it is important for our system to see if some of these proteins are concentration dependent and we can sort them from the GFP intensity. In addition, we were validating that over-expression of these proteins does not lead to total translation shutdown, which we luckily did not see.

Firstly, we explored 4EHP recruitment to these clusters and its interaction with translation sites. At first, we could not visually see a difference in translation over time throughout the cells we were activating. The translation sites persisted over the course of the 65-minute video, and they were clearly colocalizing with the clusters we formed allowing us to address that it was consistently interacting in the general location of the translation sites that were also localized. We further analyzed these videos through the same code that can extract the intensity of each individual translation site over time. Here we tracked the intensity over time, still normalizing to the first time point. Initially, the graph did not seem conclusive, there were random cells that seemed to start activating translation because the intensity measurement would increase over time. After seeing this graph, we sorted the cells based on GFP intensity, this would give us insights into the expression level of 4EHP and if this would cause these variable effects. Once sorting expression wise, there was a clear pattern in higher expressing cells beginning to turn translation on. This led us to explore the literature where we found that the HIF-2∝ factor can form a complex with 4EHP in hypoxic conditions to start initiating translation. (30) We hypothesize that in the condition we are creating in the cell some transcript

may not be accessible by normal initiation factors leading HIF-2∝ to bind 4EHP and starting initiating. This has yet to be further explored but was an incredible result of this experiment. Further experiments were done over expressing 4EHP and these provided more variable results, there is most likely a certain expression that is required for these effects. For instance, once all the Cry2 proteins are taken by 4EHP they are less likely to recruit our transcript, thus our translation sites are not stably interacting with the factors that we want them to. We then considered the fact that 4EHP bound by GIGYF2 promotes its translation shut-down capabilities. This led us to mutate the binding interface between this complex and assessing the translation effects over time. This shows consistent translation initiation, more so than the other experiments. While this is incredibly preliminary, it is promising that this mutation will promote initiation. To assess well localization of translation to these clusters are occurring we further analyzed some specific moves that had striking phenotypes. Firstly, as mentioned with our highly induced 4EHP cells, we wanted to see if our translation was successfully colocalizing when there were no effects on translation. From this breakdown we found an incredibly low percentage of translation sites recruited to these clusters when 4EHP was in abundance. As mentioned previously, there is a chance that all the GFP-nanobodies were taken up from 4EHP. When addressing a cell that had an aggressive phenotype, we do see a much higher percentage of translation colocalized to our Cry2olig cells and 4EHP GFP. There are still many questions to be answered that could be further validated through various experiments that will be described in future directions.

After exploring 4EHP's effects on translation, we moved to its upstream binder GIGYF2. GIGYF2 is first recruited by ZNF598 and then recruits the cap binding protein 4EHP. We initially hypothesized this would have the most effects on translation because it leads to

multidimensional translation shut down over time since it can also interact with the ccr/not complex, another degradation pathway of mRNA. Using our GIGYF2 stable cell line, we used the same protocol we have been using for all these experiments. Upon visual analysis there were multiple cells that completely shut down in translation with the 65 minutes we imaged for. This was exactly what we were hoping to see, however, to further analyze this data we processed the videos and analyzed them using our particle detection code. Upon generating a graph of all our GIGYF2 proteins we got highly inconclusive data, like 4EHP's. While there were a lot of cells that seemingly had their translation completely shut down, there were multiple not shut down at all. We sorted these cells based on GFP expression once more and our results were even more confounding, there were no set expression dependencies on results. This experiment was repeated multiple times with different inductions of protein expression. When GIGYF2 was highly expressed, there was even less change in translation sites over time. We investigated the colocalization of translation sites with Cry2olig and the GFP signal of GIGYF2. When GIGYF2 was highly induced we still saw this consistent colocalization of translation to the sites despite having no effects on translation. We then looked at those that had a severe response and shut down to translation and this compared to the cell that had little to no response. All in all, there seems to be consistent recruitment despite no effects on translation. Further experimentation is required to validate what is exactly occurring in the cells. There are most likely other factors required in the process that will allow GIGYF2 to have some effect on translation. In our future directions we outline multiple future experiments we are hoping to follow up and get more results from GIGYF2.

4.3 Closing remarks

As a closing remark, I believe that we have developed an integral technique for characterizing mRNA associating proteins. Through this system, any factor can be GFP-tagged and recruited to these phase-separated locations within the cells to measure effects on translation dynamics over time. This can be particularly useful for proteins with little-known functions, as it may shed light on how they affect translation, which is currently unknown. Furthermore, further characterization of the RQC pathway has raised more questions about the proposed model than before. For instance, if 4EHP can function as an initiation factor, does it require GIGYF2 to act as an inhibitor? Additionally, why is GIGYF2 recruitment on its own not leading to translation shutdown over time? These are questions that, with further experimentation, we can delve into and deconvolve. Discovering the true series of proteins involved in the pathway can significantly contribute to our understanding of this rescue machinery. This understanding is crucial, as without it, it could lead to neurodegenerative disorders in patients.

Chapter 5: Future Directions

Given the technique-based nature of this thesis, there are many future directions for this and further experiments to validate what is already concluded.

Aim 1:

My aim 1 was primarily about validating the novelty of our technique. While this worked extensively well using the Cry2olig proteins and clustering technique, there is another clustering system known as light-activated reversible inhibition by assembled trap (LARIAT). This clustering technique adds a scaffold CIB1 multimeric protein to create more lattice-like clusters within the cells. This technique was found to cause translation inhibition, however, our preliminary findings from overnight imaging indicate that translation can persist for long periods of time during activation. This was validated through puromycin treatment to validate the translation sites. We hypothesize this is due to our reporter being much larger than previous studies'. This means our reporter cannot be fully sequestered into the clusters. Moving forward, we could use this technique and determine if the clustering has a direct impact on our localization of proteins and their interactions. In addition, our transcripts have a tev sight meaning we could eventually pull them down and analyze them through mass spectrometry. This would characterize what is interacting with our clusters along with validating that our proteins of interest are interacting with the transcripts if we see translation shutdown. This could also be assessed through fixing out cells and staining for the specific proteins to visualize under our confocal microscope. With future optimization, we will be able to validate a plethora of factors that recruit to translation over time.

Aim 2:

My second aim produced a lot of answers as well as many questions. While the RQC pathway has not been starkly characterized, the current model has been heavily researched. Despite this, our findings question some of these working components as well as their ability to function on their own as translation repressors. Previously, it was found that 4EHP and GIGYF2 can function in a separate inhibition pathway from ZNF598, however, with our single recruitments of the proteins we do not see this. In fact, when we recruit 4EHP we end up seeing some initiation of translation occur due to higher translation signals over the 65-minute movies. This is something we can explore more through generating a plasmid that can bring both 4EHP and GIGYF2 to our translation sites and validate that they work better together than separate. This plasmid has been generated, it has yet to be successfully tested. In addition, since we know 4EHP can function as a translation initiation factor when complexed with HIF-2∝, we could always fix these cells and stain the presence of HIF-2∝ in our clusters to validate complexes potentially occurring. This could also be done through mass spectrometry experiments. In addition, we are looking to induce hypoxic conditions with cobalt (II) chloride in the cell and if this reflects our cluster's ability to initiate this would be interesting.

In addition to further exploration into 4EHP, we hope to further deconvolve the data we found for GIGYF2. This could be remedied through recruiting known translation suppressors to our clustered translation sites, for instance, the P-body protein argonaut. This has previously been shown to shut down translation over time through direct tethering. If this were to easily shut down translation, then we would know GIGYF2 must require more components to shut down. Furthermore, we have constructed a P2A plasmid that expresses both 4EHP and GIGYF2. With both tethered together they should function the same way that previous studies have found when recruiting both components.

Closing remarks:

All in all, there are numerous avenues that this research could lead us down. For instance, in the future, we hope to investigate stress granule scaffolds and determine if their recruitment causes adverse effects on our translation sites over time. Additionally, we aim to better compare the cluster-like ability of Cry2 versus G3BP1. Furthermore, we plan to conduct further experiments into the recruitment of p-body proteins such as argonaut. With continued optimization of the system, this technique will become indispensable for the lab to discover additional functions of proteins.

Chapter 6: Materials and Methods

Plasmid Construction

All vectors were designed through the Snapgene software. Our Cry2olig plasmids were cloned through inputting the Cry2 protein into an expression vector with a CMV promoter and placing the Snaptag on the 5' end along with the GFP-nanobody (vhH(GFP)) on the 3' end of the protein. This is the construct we consistently used throughout our experiment involving the blue light sensitive protein. In addition, we developed a plasmid that can be transfected to express the HAscFV and MCP separated by an IRES. We used the Frankenbody scFV and inserted that before the IRES. Our 2 MCP sequence still included a Halotag before it. A GB1 sequence was placed after the frankenbody. This plasmid was kanamycin resistant. This was used for all of our assays.

Our proteins of interest were each tagged with a GFP upstream of their protein sequence. These were designed with D3 promoters because it was the goal to express these in stable cell lines. The protein sequences were obtained from GeneWiz. These were constructed with ampicillin resistance. In addition, we developed the constructs separated by a P2A sequence. This was placed in between the two proteins as such: GFP-4EHP-P2A-GFP-GIGYF2. These were all done through standard restriction enzyme cloning and developing specific primers. On the side we also generated GFP-Ago2 in the same fashion described above. All our primers were tested on the Integrated DNA Technologies (IDT) database. All our plasmids were sequenced using full plasmid sequencing offered by Plasmidsaurus. All cloning was done using Zymo Research miniprep and gel extraction kits. Some plasmids were midi-prepped using the machinery-nagel kit.

Cell Culture:

Human osteosarcoma cells (U2OS) were used for most of these images. For those indicated, we used HeLa generated stable cell lines as well. These were cultured in 10% (v/v) FBS (Atlas) media DMEM (Thermo Scientific) supplemented with 1 mM L-glutamine (Gibco) and 1% (v/v) Pen/Strep (Invitrogen/Gibco) and grown at 37 °C in 5% CO2. These were kept at a confluence between 20% and 80% before passing. The original stock of U2OS were purchased from ATCC and STP profiled in addition to morphological assessments. These were then ensured to not have mycoplasma contaminations.

Stable Cell Line Generation:

The stable cell lines used stably expressed Cry2olig, GIGYF2, and 4EHP. We used the piggybac method which utilizes transposons in the genetic code to input our genes of interest. We cloned our protein of interest into the piggybac vector and transfected the components along with a transposase. This generated polyclonal stable cells lines we then used for further experiments. Stable transfections were done overnight to fully integrate our components into the transposons within the DNA. After 12-24 hours, the transfection material was washed out and antibiotic selection began. These components were selected for using 0.75 ul of 200ul G148. They were fully selected after 5 days and left to grow back up. If necessary, a second round of selection can be done. The integrated components are inducible through doxycycline, and this was how we tested the efficiency of our stable cell line generation and selection.

Transfection:

Transfections were used to integrate all our components into our cells. This was done using the LTX Lipofectamine with Plus reagent kit (thermofisher), following manufacturer's protocol. In

total, we would add 1.5 ug of DNA which required a total of 145 ul of Opti-MEM, 4.5 ul of LTX, and 1.5 ul of the P reagent. These components are then mixed and left to sit for 5 minutes. This was then added to a 10 mm MatTek chamber dish holding 1 ml of our DMEM media described in cell culture sections with our cells at 80% confluency. This was left to incubate overnight and washed out after 6-8 hours. When imaging Cry2Olig, only 1000 ng of reporter, and 200 ng of HA scFV were used. When imaging GIGYF2 and 4EHP stable cell lines, 1000 ng of reporter, 200 ng of HAscFV reporter, and 250 ng of Cry2olig was used. When imaging the mutants in our Cry2olig stable cell line, 250 ng of GIGYF2_mut and 4EHP_mut were used along with our Ago2 experiment.

Cell Imaging with Hilo Microscope:

Live-cell imaging was executed using a specially crafted widefield fluorescence microscope with an innovative highly inclined thin illumination setup, previously described. This microscope utilizes three lasers (488, 561, and 637 nm from Vortran) for excitation, a 60X objective lens with a numerical aperture of 1.49 for oil immersion (Olympus), an emission image splitter (T660lpxr, ultra-flat imaging grade, Chroma), and twin EMCCD cameras (iXon Ultra 888, Andor). For optimal Nyquist sampling, achromatic doublet lenses with a 300 mm focal length (AC254-300-A-ML, Thorlabs) were employed to focus images onto the camera chips, deviating from the conventional 180 mm Olympus tube lens. This lens combination delivers 100X images with a resolution of 130 nm/pixel. The imaging configuration involved capturing the far-red signal of Cry2Olig, visualized by JF646 Snaptag-Cry2, on one camera, while the green signal of translation, visualized by HA scFV frank body, and the blue signal of GFP-tagged proteins of interests, GIGYF2, 4EHP, or Ago-2 were recorded on the second camera. To mitigate signal bleed-through between the red and green channels, a high-speed filter wheel (HS-625 HSFW

TTL, Finger Lakes Instrumentation) featuring specific filters (593/46 nm BrightLine for red and 510/42 nm BrightLine for green, Semrock) was strategically placed in front of the second camera. Maintaining focus during experiments was achieved through the CRISP Autofocus System (CRISP-890, Applied Scientific Instrumentation), and Z-stack images were obtained using a piezoelectric stage (PZU-2150, Applied Scientific Instrumentation). Synchronization of laser emission, camera integration, piezoelectric stage movement, and emission filter wheel position change was orchestrated by an Arduino Mega board (Arduino). The entire image acquisition process was orchestrated using the open-source Micro-Manager software (version 1.4.22). To initiate live-cell imaging, live cells were introduced into a stage-top environmental chamber maintained at 37 °C with 5% CO2 (Okolab), allowing for a 30-minute equilibration period before image acquisition. Parameters such as imaging size, exposure time, and vertical shift speed were configured at 512 × 512 pixels², 53.64 msec, and 1.13 microseconds, respectively, resulting in an imaging rate of 13 Hz (70 msec per image). To encompass the entire cytoplasmic thickness of U2OS cells, a total of 13 Z-stacks with a step size of 500 nm were captured, wherein the Z-position changed every 2 images for both the red and green signals within each stack. This approach yielded a maximal cellular imaging rate of 0.5 Hz (2 sec per volume). For instances requiring lower frame rates, delays between volume captures were implemented. For prolonged single-molecule tracking, aimed at minimizing photobleaching, Cry2olig (JF646) and translation (HA scFV) were imaged every 1 minute, while imaging tethered proteins of interest (GFP) were imaged every 5 timepoints. Laser powers for all recorded sequences were carefully controlled, set at 10-15 mW for 637 nm, 1-5 mW for 488 nm, and 13-15 mW for 561 nm, with an ND10 neutral density filter set at the beam expander.

At the conclusion of each imaging session, TetraSpeck Fluorescent Microspheres (100 nm, Thermo Fisher Scientific) affixed to a MatTek chamber underwent imaging to rectify the subtle misalignment between the two cameras. The acquired bead images were then employed to construct a transformation matrix using the Projective Transform function within the scikit-image library in Python. This matrix served to correct any offsets observed in the detected particle positions within each channel.

Image Analysis:

After capturing our movies, they needed to be processed for proper analysis through our developed pipeline. Before further processing, we needed to sort our image stacks based on the color each laser was exciting our fluorophores with. This is all done in the ImageJ (FJI) software which can separate our channels into three colors and organize them accordingly. Once these processed videos are generated, we can move to our coding pipeline.

Our videos are processed through our pipeline developed in Python coding software. For simplicity, it is separated into four separate steps. We begin with pre-processing which requires you to load your bead images in and develop a matrix that you can align the cameras with. The next steps involve the photo bleach correction. To avoid artifact loss of intensity, we correct for any potential photobleaching through normalizing intensities to the first time point. This is important because we are tracking translation intensity over time, without the photo bleach correction it may appear these spots are disappearing overtime or dimming. This is also included with a background subtraction stage that helps us reduce noise as much as possible for the future steps of analysis. This photobleached corrected video is saved and used from here on out. The next step is our particle detection. This is done through masking our cells and setting a threshold

that will identify all our higher intensity translation sites, but not pick up on any background noise. This then uses a disk and donut technique to subtract the background around it within the same channel and get the raw intensity of the translation site. This happens all at once in one cell once you mask to exclude the nucleus and include the cell's cytoplasm. These particles are then all counted and normalized to the first time point. This data is then saved and used in our final section of quantifying translation intensity over time. Our fourth and final step allows us to take all our processed data and graph them according to the first normalized time point. This allows us to compare cells with differing starting translation sites which is useful in getting more replicates of our experiments. This is where our final figures come from and help us further develop our results through this quantitative analysis. For instance, our final step has been to measure the intensity of the clusters recruiting our translation sites and deciphering whether this plays a role in translation recruitment. In addition, we are tracking the intensity of GFP in these clusters. This indicates how much our proteins of interest will be expressed; this is easily changed within the code because we can measure for different specific channels. Further optimization of this code will occur for us to get the most information out of our data that we can.

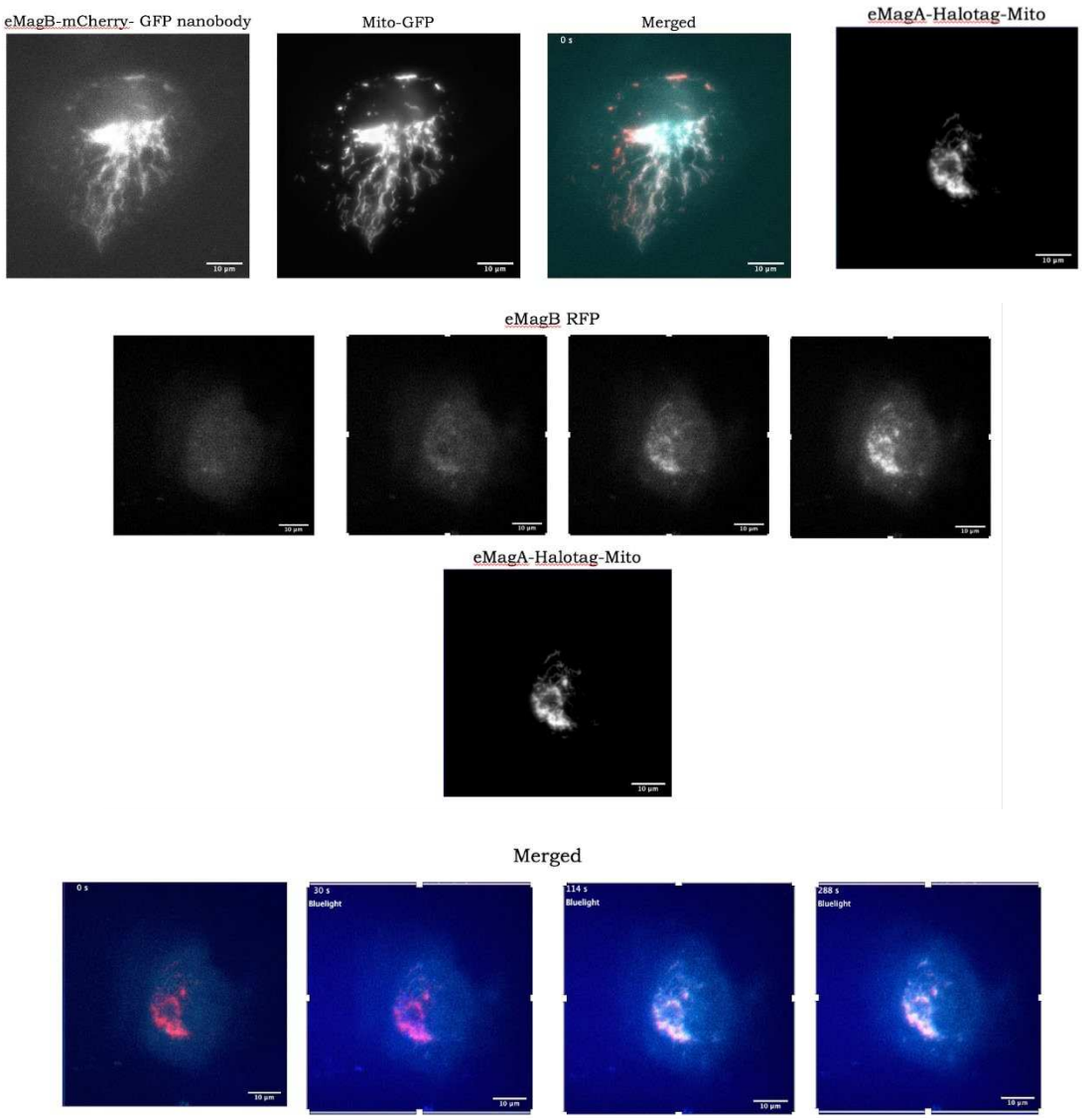

Figure 9: Tethering control of the eMag system

A, Recruitment of eMagB-mCherry-GFPnanobody to the GFP tagged mito signals. **B,** eMagB-RFP recruitment to eMagA after blue-light signal. **C,** eMagA localized to mitochondria giving a mitochondria signal. **D,** Merged image of eMagB and eMagA showing co-localization of intensities. White indicates overlap of blue and red signals.

Enhanced magnet system

Our preliminary data suggest that the eMag system can effectively tether eMagB to eMagA in vivo. To ensure tethering control, we placed a mitochondrial localization protein on one of our enhanced magnet proteins, eMagB (Figure 9A). In addition to tagging eMagB, we tagged the mitochondria with a GFP. With both components tagged, we can see an overlap of our red and blue signals in white indicating colocalization. Next, we applied the tethering system the enhanced magnets are capable of. In another cell, we placed the mitochondrial localizing signal on eMagA and had our eMagB freely diffuse with no localization signal but tagged with a red fluorescent protein (RFP) (Figure 9B, C, D). Upon blue light exposure, eMagB is quickly recruited to the eMagA signal. We can see colocalization over time in our merged channel timelapse, the white once again indicating an overlap of red and blue signals. Despite the tethering system effectively working, translation signal recruitment was not tested. It was discovered that to visualize our translation signal along with protein recruitment, we would need access to an additional imaging channel to tag four components. We were attempting to visualize eMagA, eMagB, translation signals, and RQC protein recruitment, however, we only have three light channels to view tags. Subsequently, we had to pursue a different means of tethering or colocalization of translation signals to control the local environment more effectively and efficiently with our options given by the microscope. Despite its novel implication, the eMag system was too complex to continue pursuing.

scFV generation - TerryBody:

While working through Kimura and Taguchi's lab at the Tokyo Institute of Technology, I was able to work on my protein design skills. Using AlphaFold2 and Protein MPNN, I was able to design codon optimized scFVs that target the spike protein of Covid-19. This will help screening for viruses in the future and potential drug targeting. Developing a fast efficient way to generate scFV's is integral to the promising development of biological technologies. [43,44]

Citations

1. CRICK FH. On protein synthesis. Symp Soc Exp Biol. 1958;12:138-63. PMID: 13580867.
2. Brenner S, Jacob F, Meselson M. An unstable intermediate carrying information from genes to ribosomes for protein synthesis. Nature. 1961 May 13;190:576-581. doi: 10.1038/190576a0. PMID: 20446365.
3. Gros F, Hiatt H, Gilbert W, Kurland CG, Risebrough RW, watson JD. Unstable ribonucleic acid revealed by pulse labelling of Escherichia coli. Nature. 1961 May 13;190:581-5. doi: 10.1038/190581a0. PMID: 13708983.
4. Pestova TV, Kolupaeva VG, Lomakin IB, Pilipenko EV, Shatsky IN, Agol VI, Hellen CU. Molecular mechanisms of translation initiation in eukaryotes. Proc Natl Acad Sci U S A. 2001 Jun 19;98(13):7029-36. doi: 10.1073/pnas.111145798. PMID: 11416183; PMCID: PMC34618.
5. Tuller T, Waldman YY, Kupiec M, Ruppin E. Translation efficiency is determined by both codon bias and folding energy. Proc Natl Acad Sci U S A. 2010 Feb 23;107(8):3645-50. doi: 10.1073/pnas.0909910107. Epub 2010 Feb 2. PMID: 20133581; PMCID: PMC2840511.
6. Xu B, Liu L, Song G. Functions and Regulation of Translation Elongation Factors. Front Mol Biosci. 2022 Jan 19;8:816398. doi: 10.3389/fmolb.2021.816398. PMID: 35127825; PMCID: PMC8807479.
7. Ceci, M., Gaviraghi, C., Gorrini, C. *et al.* Release of eIF6 (p27BBP) from the 60S subunit allows 80S ribosome assembly. *Nature* 426, 579–584 (2003). https://doi.org/10.1038/nature02160

8. Jurado AR, Tan D, Jiao X, Kiledjian M, Tong L. Structure and function of pre-mRNA 5'-end capping quality control and 3'-end processing. Biochemistry. 2014 Apr 1;53(12):1882-98. doi: 10.1021/bi401715v. Epub 2014 Mar 20. PMID: 24617759; PMCID: PMC3977584.
9. Sonenberg N. eIF4E, the mRNA cap-binding protein: from basic discovery to translational research. Biochem Cell Biol. 2008 Apr;86(2):178-83. doi: 10.1139/O08-034. PMID: 18443631.
10. Li W, Belsham GJ, Proud CG. Eukaryotic initiation factors 4A (eIF4A) and 4G (eIF4G) mutually interact in a 1:1 ratio in vivo. J Biol Chem. 2001 Aug 3;276(31):29111-5. doi: 10.1074/jbc.C100284200. Epub 2001 Jun 14. PMID: 11408474.
11. Sonneveld S, Verhagen BMP, Tanenbaum ME. Heterogeneity in mRNA Translation. Trends Cell Biol. 2020 Aug;30(8):606-618. doi: 10.1016/j.tcb.2020.04.008. Epub 2020 May 25. PMID: 32461030.
12. Kolitz SE, Lorsch JR. Eukaryotic initiator tRNA: finely tuned and ready for action. FEBS Lett. 2010 Jan 21;584(2):396-404. doi: 10.1016/j.febslet.2009.11.047. PMID: 19925799; PMCID: PMC2795131.
13. Hershey JWB, Sonenberg N, Mathews MB. Principles of Translational Control. Cold Spring Harb Perspect Biol. 2019 Sep 3;11(9):a032607. doi: 10.1101/cshperspect.a032607. PMID: 29959195; PMCID: PMC6719596.
14. Kershaw CJ, Nelson MG, Castelli LM, Pavitt GD, Hubbard SJ, Ashe MP. Journal of Biological Chemistry. 2023 Oct; 299(10) 105195. Doi: https://doi.org/10.1016/j.jbc.2023.105195

15. Joazeiro CAP. Mechanisms and functions of ribosome-associated protein quality control. Nat Rev Mol Cell Biol. 2019 Jun;20(6):368-383. doi: 10.1038/s41580-019-0118-2. PMID: 30940912; PMCID: PMC7138134.
16. Yan X, Hoek TA, Vale RD, Tanenbaum ME. Dynamics of Translation of Single mRNA Molecules In Vivo. Cell. 2016 May 5;165(4):976-89. doi: 10.1016/j.cell.2016.04.034. PMID: 27153498; PMCID: PMC4889334.
17. Wu B, Eliscovich C, Yoon YJ, Singer RH. Translation dynamics of single mRNAs in live cells and neurons. Science. 2016 Jun 17;352(6292):1430-5. doi: 10.1126/science.aaf1084. Epub 2016 May 5. PMID: 27313041; PMCID: PMC4939616.
18. Pichon X, Bastide A, Safieddine A, Chouaib R, Samacoits A, Basyuk E, Peter M, Mueller F, Bertrand E. Visualization of single endogenous polysomes reveals the dynamics of translation in live human cells. J Cell Biol. 2016 Sep 12;214(6):769-81. doi: 10.1083/jcb.201605024. Epub 2016 Sep 5. PMID: 27597760; PMCID: PMC5021097.
19. Morisaki T, Lyon K, DeLuca KF, DeLuca JG, English BP, Zhang Z, Lavis LD, Grimm JB, Viswanathan S, Looger LL, Lionnet T, Stasevich TJ. Real-time quantification of single RNA translation dynamics in living cells. Science. 2016 Jun 17;352(6292):1425-9. doi: 10.1126/science.aaf0899. Epub 2016 May 5. PMID: 27313040.
20. Morisaki T, Lyon K, DeLuca KF, DeLuca JG, English BP, Zhang Z, Lavis LD, Grimm JB, Viswanathan S, Looger LL, Lionnet T, Stasevich TJ. Real-time quantification of single RNA translation dynamics in living cells. Science. 2016 Jun 17;352(6292):1425-9. doi: 10.1126/science.aaf0899. Epub 2016 May 5. PMID: 27313040.
21. Zhao N, Kamijo K, Fox PD, Oda H, Morisaki T, Sato Y, Kimura H, Stasevich TJ. A genetically encoded probe for imaging nascent and mature HA-tagged proteins in vivo.

Nat Commun. 2019 Jul 3;10(1):2947. doi: 10.1038/s41467-019-10846-1. PMID: 31270320; PMCID: PMC6610143.

22. Aguilera LU, Raymond W, Fox ZR, May M, Djokic E, Morisaki T, Stasevich TJ, Munsky B. Computational design and interpretation of single-RNA translation experiments. PLoS Comput Biol. 2019 Oct 16;15(10):e1007425. doi: 10.1371/journal.pcbi.1007425. PMID: 31618265; PMCID: PMC6816579.
23. Grünwald D, Singer RH. In vivo imaging of labelled endogenous β-actin mRNA during nucleocytoplasmic transport. Nature. 2010 Sep 30;467(7315):604-7. doi: 10.1038/nature09438. Epub 2010 Sep 15. PMID: 20844488; PMCID: PMC3005609.
24. Li W, Maekiniemi A, Sato H, Osman C, Singer RH. An improved imaging system that corrects MS2-induced RNA destabilization. Nat Methods. 2022 Dec;19(12):1558-1562. doi: 10.1038/s41592-022-01658-1. Epub 2022 Nov 10. PMID: 36357695; PMCID: PMC7613886.
25. Cialek CA, Galindo G, Morisaki T, Zhao N, Montgomery TA, Stasevich TJ. Imaging translational control by Argonaute with single-molecule resolution in live cells. Nat Commun. 2022 Jun 10;13(1):3345. doi: 10.1038/s41467-022-30976-3. PMID: 35688806;
26. Cialek CA, Koch AL, Galindo G, Stasevich TJ. Lighting up single-mRNA translation dynamics in living cells. Curr Opin Genet Dev. 2020 Apr;61:75-82. doi: 10.1016/j.gde.2020.04.003. Epub 2020 May 11. PMID: 32408104; PMCID: PMC7508770.PMCID: PMC9187665.

27. Taslimi, A., Vrana, J., Chen, D. *et al.* An optimized optogenetic clustering tool for probing protein interaction and function. *Nat Commun* 5, 4925 (2014). https://doi.org/10.1038/ncomms5925

28. Che DL, Duan L, Zhang K, Cui B. The Dual Characteristics of Light-Induced Cryptochrome 2, Homo-oligomerization and Heterodimerization, for Optogenetic Manipulation in Mammalian Cells. ACS Synthetic Biology 2015 4(10). 1124-1135. https://doi.org/10.1021/acssynbio.5b00048

29. Benedetti L, Marvin JS, Falahati H, Guillén-Samander A, Looger LL, De Camilli P. Optimized Vivid-derived Magnets photodimerizers for subcellular optogenetics in mammalian cells. Elife. 2020 Nov 11;9:e63230. doi: 10.7554/eLife.63230. PMID: 33174843; PMCID: PMC7735757.

30. Park H, Kim NY, Lee S, Kim N, Kim J, Heo WD. Optogenetic protein clustering through fluorescent protein tagging and extension of CRY2. Nat Commun. 2017 Jun 23;8(1):30. doi: 10.1038/s41467-017-00060-2. PMID: 28646204; PMCID: PMC5482817.

31. Lee S, Park H, Kyung T, Kim NY, Kim S, Kim J, Heo WD. Reversible protein inactivation by optogenetic trapping in cells. Nat Methods. 2014 Jun;11(6):633-6. doi: 10.1038/nmeth.2940. Epub 2014 May 4. PMID: 24793453.

32. Kim NY, Lee S, Yu J, Kim N, Won SS, Park H, Heo WD. Optogenetic control of mRNA localization and translation in live cells. Nat Cell Biol. 2020 Mar;22(3):341-352. doi: 10.1038/s41556-020-0468-1. Epub 2020 Feb 17. PMID: 32066905.

33. Liu R, Fang M, Chen X, Yang Y. The status and challenges of optogenetic tools for precise spatiotemporal control of RNA metabolism and function. Clin Transl Med. 2022 Oct;12(10):e1078. doi: 10.1002/ctm2.1078. PMID: 36245329; PMCID: PMC9574486.

34. Osswald M, Santos AF, Morais-de-Sá E. Light-Induced Protein Clustering for Optogenetic Interference and Protein Interaction Analysis in *Drosophila* S2 Cells. Biomolecules. 2019 Feb 12;9(2):61. doi: 10.3390/biom9020061. PMID: 30759894; PMCID: PMC6406598.

35. Hickey KL, Dickson K, Cogan JZ, Replogle JM, Schoof M, D'Orazio KN, Sinha NK, Hussmann JA, Jost M, Frost A, Green R, Weissman JS, Kostova KK. GIGYF2 and 4EHP Inhibit Translation Initiation of Defective Messenger RNAs to Assist Ribosome-Associated Quality Control. Mol Cell. 2020 Sep 17;79(6):950-962.e6. Doi:

36. Zinshteyn B, Sinha NK, Enam SU, Koleske B, Green R. Translational repression of NMD targets by GIGYF2 and EIF4E2. PLoS Genet. 2021 Oct 19;17(10):e1009813. doi: 10.1371/journal.pgen.1009813. PMID: 34665823; PMCID: PMC8555832.

37. Hersch SJ, Elgamal S, Katz A, Ibba M, Navarre WW. Translation initiation rate determines the impact of ribosome stalling on bacterial protein synthesis. J Biol Chem. 2014 Oct 10;289(41):28160-71. doi: 10.1074/jbc.M114.593277. Epub 2014 Aug 22. PMID: 25148683; PMCID: PMC4192472.

38. Tesina P, Lessen LN, Buschauer R, Cheng J, Wu CC, Berninghausen O, Buskirk AR, Becker T, Beckmann R, Green R. Molecular mechanism of translational stalling by inhibitory codon combinations and poly(A) tracts. EMBO J. 2020 Feb 3;39(3):e103365. doi: 10.15252/embj.2019103365. Epub 2019 Dec 20. PMID: 31858614; PMCID: PMC6996574.

39. Amaya Ramirez CC, Hubbe P, Mandel N, Béthune J. 4EHP-independent repression of endogenous mRNAs by the RNA-binding protein GIGYF2. Nucleic Acids Res. 2018 Jun 20;46(11):5792-5808. doi: 10.1093/nar/gky198. PMID: 29554310; PMCID: PMC6009589.

40. Christie M, Igreja C. eIF4E-homologous protein (4EHP): a multifarious cap-binding protein. FEBS J. 2023 Jan;290(2):266-285. doi: 10.1111/febs.16275. Epub 2021 Nov 29. PMID: 34758096.

41. Melanson G, Timpano S, Uniacke J. The eIF4E2-Directed Hypoxic Cap-Dependent Translation Machinery Reveals Novel Therapeutic Potential for Cancer Treatment. Oxid Med Cell Longev. 2017;2017:6098107. doi: 10.1155/2017/6098107. Epub 2017 Nov 26. PMID: 29317983; PMCID: PMC5727761.

42. Christie M, Igreja C. eIF4E-homologous protein (4EHP): a multifarious cap-binding protein. FEBS J. 2023 Jan;290(2):266-285. doi: 10.1111/febs.16275. Epub 2021 Nov 29. PMID: 34758096.

43. Shirai YT, Suzuki T, Morita M, Takahashi A, Yamamoto T. Multifunctional roles of the mammalian CCR4-NOT complex in physiological phenomena. Front Genet. 2014 Aug 21;5:286. doi: 10.3389/fgene.2014.00286. PMID: 25191340; PMCID: PMC4139912.

44. Dauparas J, Anishchenko I, Bennett N, Bai H, Ragotte RJ, Milles LF, Wicky BIM, Courbet A, de Haas RJ, Bethel N, Leung PJY, Huddy TF, Pellock S, Tischer D, Chan F, Koepnick B, Nguyen H, Kang A, Sankaran B, Bera AK, King NP, Baker D. Robust deep learning-based protein sequence design using ProteinMPNN. Science. 2022 Oct 7;378(6615):49-56. doi: 10.1126/science.add2187. Epub 2022 Sep 15. PMID: 36108050; PMCID: PMC9997061.

45. Jumper J, Evans R, Pritzel A, Green T, Figurnov M, Ronneberger O, Tunyasuvunakool K, Bates R, Žídek A, Potapenko A, Bridgland A, Meyer C, Kohl SAA, Ballard AJ, Cowie A, Romera-Paredes B, Nikolov S, Jain R, Adler J, Back T, Petersen S, Reiman D, Clancy E, Zielinski M, Steinegger M, Pacholska M, Berghammer T, Bodenstein S, Silver D, Vinyals O, Senior AW, Kavukcuoglu K, Kohli P, Hassabis D. Highly accurate protein structure prediction with AlphaFold. Nature. 2021 Aug;596(7873):583-589. doi: 10.1038/s41586-021-03819-2. Epub 2021 Jul 15. PMID: 34265844; PMCID: PMC8371605.